



SAPIENZA
UNIVERSITÀ DI ROMA

FACOLTÀ DI INGEGNERIA DELL'INFORMAZIONE, INFORMATICA E STATISTICA

LOCOMOTION AND HAPTIC INTERFACES FOR VR EXPLORATION

**Vibration Suppression Design for Virtual Compliance
Control in Bilateral Teleoperation**

Professor

Alessandro De Luca

Students

Edoardo Ghini

Gianluca Cerilli

Giuseppe L'Erario

Academic Year 2017/2018

Contents

| | | |
|----------|---|-----------|
| 1 | System Modeling | 4 |
| 2 | Simulations | 8 |
| 2.1 | Disturbance rejection performances | 9 |
| 2.2 | Task execution analysis | 12 |
| 2.2.1 | Free motion with high noise frequencies | 12 |
| 2.2.2 | Free motion with low noise frequencies | 12 |
| 2.2.3 | Environment contact | 12 |
| 3 | Conclusions | 17 |

Introduction

Teleoperation extends the human capability to manipulating objects remotely. An important aspect deals with necessity to obtain, on operator side, similar condition as those at the remote location, in other words, a *properly(?)* feedback.

A bilateral system is composed by a joystick, called *master*, on the human side, connected to a *slave* on the environment side.

The human imposes a force on the master, that results in a displacement. This displacement is then transmitted to the slave. On the other side, literally (ahah!), the slave has a force sensor used to "send back" to the master the reflection forces at the environment side. For these reasons we can call it *bilateral teleoperation*.

Two important goals of the teleoperation are [1]:

- **Stability** of the closed loop system irrespective to the behavior of the human and the environment;
- **Transparency** of the teleoperation task: we want forces and displacements be the same on the two sides of the system.

Stability of the system can be ruined by unwanted disturbance, internal and external:

- **Internal disturbance**, due to the uncertainties in modeling of the system;
- **External disturbance**, such as unexpected input contaminated with vibration noise from both sides of the system.

This report deals with the development of a controller able to suppress the vibration and unwanted inputs in a bilateral control system [2].

In particular, the work is based on the concept of one degree of freedom inertia-spring-damper system. This concept comes from the design of shock absorbers used in vehicle suspension (which is composed by a spring and damper), and is usually applied in bilateral control system for *soft manipulation*.

Here, it is used a spring-damper system with an additional inertia. The disturbance suppression performances depends on the value of these virtual parameters, determined from the desired cut-off frequencies.

The report is organized as follow: in the first part we model the inertia-spring-damper system, analyzing the proposed control and the hybrid matrix. Then is the described the virtual parameter selection process. Finally, we present the results obtained in the simulations, performed with Matlab and Simulink.

1 System Modeling

Nomenclature

- J_m = inertia of the master, kg m^2 ;
- J_s = inertia of the slave, kg m^2 ;
- J_{mv} = virtual inertia of the master, kg m^2 ;
- J_{sv} = virtual inertia of the slave, kg m^2 ;
- B_v = virtual damping of the system, $\frac{\text{N m}}{\text{rad/s}}$;
- K_v = virtual spring of the system, $\frac{\text{N m}}{\text{rad}}$;
- τ_m = master torque, N m ;
- θ_m = master displacement, rad ;
- τ_s = slave torque, N m ;
- θ_s = slave displacement, rad ;

Modeling

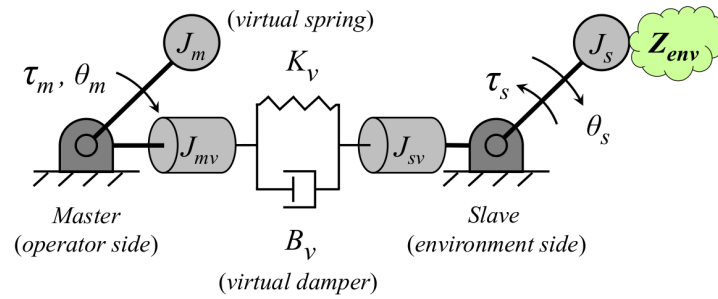


Figure 1: Spring-damper-inertia system with virtual parameters.

The inertia-spring-damping system is shown in Fig.1: the master and the slave have the real inertia J_m and J_s and the virtual ones J_{mv} and J_{sv} . Master and slave are interconnected with the virtual damper B_v and the virtual spring K_v .

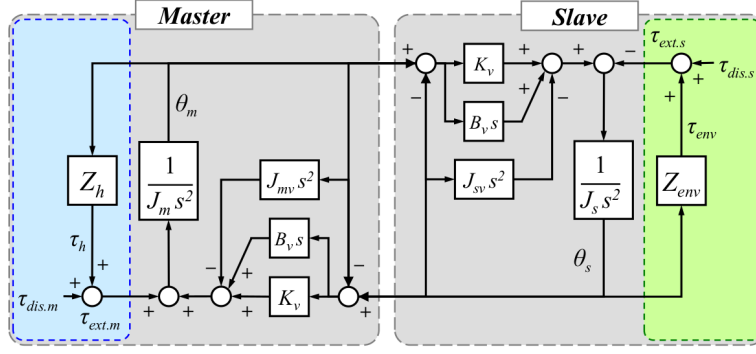


Figure 2: Block diagram of the bilateral control system.

The dynamic equation of the system are:

$$(J_m + J_{mv})\ddot{\theta}_m + B_v(\dot{\theta}_m - \dot{\theta}_s) + K_v(\theta_m - \theta_s) = \tau_m \quad (1)$$

$$(J_s + J_{sv})\ddot{\theta}_s + B_v(\dot{\theta}_s - \dot{\theta}_m) + K_v(\theta_s - \theta_m) = -\tau_s \quad (2)$$

and, in frequency domain:

$$(J_m + J_{mv})s^2\theta_m + (B_v s + K_v)(\theta_m - \theta_s) = \tau_m \quad (3)$$

$$(J_s + J_{sv})s^2\theta_s + (B_v s + K_v)(\theta_s - \theta_m) = -\tau_s \quad (4)$$

The virtual parameters are considered elements of the controller. For this aim the equations above are rearranged:

$$J_m s^2 \theta_m = \tau_m - (B_v s + K_v)(\theta_m - \theta_s) - J_{mv} s^2 \theta_m \quad (5)$$

$$J_s s^2 \theta_s = -\tau_s - (B_v s + K_v)(\theta_s - \theta_m) - J_{sv} s^2 \theta_s \quad (6)$$

$$(7)$$

where the external torques are action and reaction forces of the human and the environment.

The block diagram of the proposed control system is constructed as shown in Fig.2¹.

A bilateral control can be represented by a 2x2 matrix, called *hybrid matrix*:

$$\begin{bmatrix} \tau_m \\ \theta_s \end{bmatrix} = \begin{bmatrix} H_{11} & H_{12} \\ H_{21} & H_{22} \end{bmatrix} \begin{bmatrix} \theta_m \\ -\tau_s \end{bmatrix} \quad (8)$$

¹Delay time in communication channel is not considered in the reference paper [2].

and every H_{ij} is an hybrid parameter.

In particular:

$$H_{11} = \frac{1}{Z_s} [Z_m Z_s - (B_v s + K_v)^2] \quad (9)$$

$$H_{12} = -\frac{1}{Z_s} [B_v s + K_v] \quad (10)$$

$$H_{21} = \frac{1}{Z_s} [B_v s + K_v] \quad (11)$$

$$H_{22} = \frac{1}{Z_s} \quad (12)$$

where:

$$Z_m = (J_m + J_{mv})s^2 + B_v s + K_v \quad (13)$$

$$Z_s = (J_s + J_{sv})s^2 + B_v s + K_v \quad (14)$$

The system should achieve two conditions:

- the position of both sides should be the same;
- the law of action-reaction should hold;

represented by the *transparency condition*:

$$\tau_m = \tau_s \quad (15)$$

$$\theta_m = \theta_s \quad (16)$$

is expressed in terms of transmitted impedance Z_t , which is transferred to the human, and environment impedance Z_{env} :

$$\frac{\tau_m}{\theta_m} = Z_t = Z_{env} = \frac{\tau_s}{\theta_s} \quad (17)$$

The relationship between the transmitted and environment impedance comes from the hybrid matrix of (8):

$$Z_t = \left(\frac{-H_{12}H_{21}}{1 + H_{22}Z_{env}} \right) Z_{env} + H_{11} \quad (18)$$

and, to achieve the perfect transparency condition shown in (16), the hybrid parameters should be derived as:

$$\begin{bmatrix} \tau_m \\ \theta_s \end{bmatrix} = \begin{bmatrix} 0 & -1 \\ 1 & 0 \end{bmatrix} \begin{bmatrix} \theta_m \\ -\tau_s \end{bmatrix} \quad (19)$$

The performance of a teleoperation is evaluated in *free* and *contact* motion. For free motion the external torque on the slave is usually equal to zero, and hence the only parameters affecting the transparency are H_{11} and H_{12} . For contact motion, instead, all the hybrid parameters affect the performance.

Parameter selection and design

The system is assumed to be disturbed by external vibration noise from the environment. We want to know how the slave position is affected by the external noise. This analysis can be achieved inspecting the hybrid parameter H_{22} , representing how the position responds to external torque:

$$\frac{\theta_s}{\tau_{ext}} = \frac{1}{(J_s + J_{sv})s^2 + B_v s + K_v} \quad (20)$$

The virtual parameter in (20) are determined from the second-order characteristic equation of the system:

$$(s + g_1)(s + g_2) = 0 \quad (21)$$

where the poles g_1 and g_2 represent the cut-off frequencies of the system for disturbance suppression purpose

We can determine the virtual parameters comparing the characteristic equation of (20) with (21).

The operator should feel the reflecting force from the environment vividly. Assuming for a moment we do not care about the vibration suppression, for the proposed control the system can achieve a large transparency with high spring stiffness K_v and a damping $B_v \rightarrow 0$.

It is clear that the value of spring stiffness K_v has an important influence on the transparency of the system: we want to choose it beforehand and the other virtual parameters will be calculated accordingly. The virtual damping coefficient B_v :

$$\frac{B_v}{K_v} = \frac{g_1 + g_2}{g_1 \cdot g_2} \Rightarrow B_v = \frac{g_1 + g_2}{g_1 \cdot g_2} K_v \quad (22)$$

and, in the same fashion, the virtual inertia J_{sv} :

$$J_{sv} = \frac{1}{g_1 \cdot g_2} K_v - J_s \quad (23)$$

The spring stiffness, as said before, influences the behavior of the system. Choosing it properly we can obtain:

- **rigid coupling**, with high stiff spring, obtaining an high transparency;
- **spring coupling**, when the value of the stiffness is low.

In other words we can use the spring stiffness to regulate the *compliance* of the system.

2 Simulations

In regards of the simulation scenarios we are deliberately neglecting the critical aspects of the communication between master and slave, therefore assuming ideal conditions as an instantaneous and loss-less signal transfer, without noise. The table in fig describes the parameters chosen such as inertiae and cut-off frequencies in addition to the range of values that the virtual coefficients have undertaken.

| | | | |
|-------|----------------|-------------------|---------|
| J_m | Master Inertia | $5 \cdot 10^{-4}$ | kgm^2 |
| J_s | Slave Inertia | $5 \cdot 10^{-4}$ | kgm^2 |

Table 1: Parameters adopted in simulations

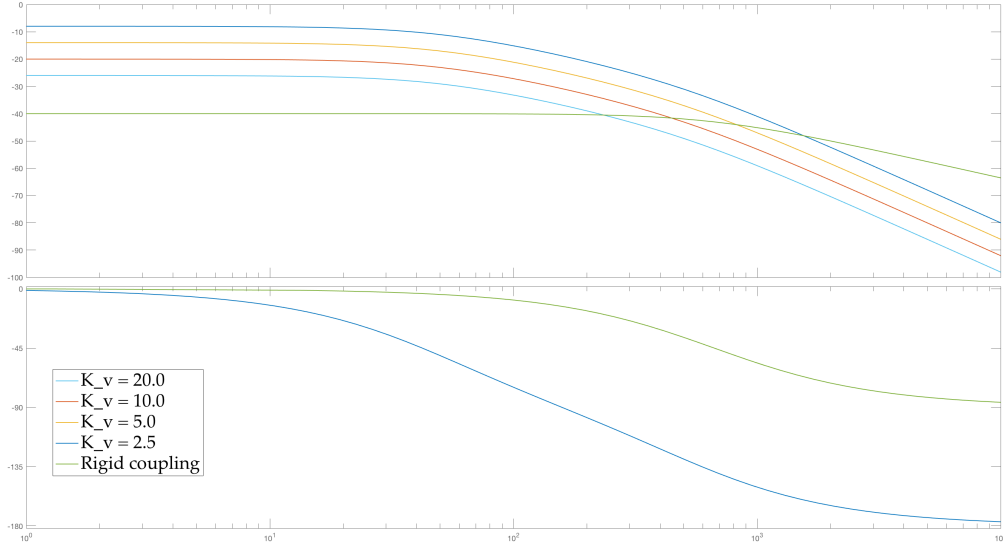


Figure 3: Bode diagram of the proposed vibration filter

2.1 Disturbance rejection performances

Considering at first the rigid coupling case, in which, as being said, almost full transparency is achieved between master and slave, henceforth the vibrations generated slave-side will be felt almost with the same intensity by master-side whatever would be the vibration frequency.

For this reason, in order to reach better task execution performances we want to reduce the impact of environment vibrations at minimum.

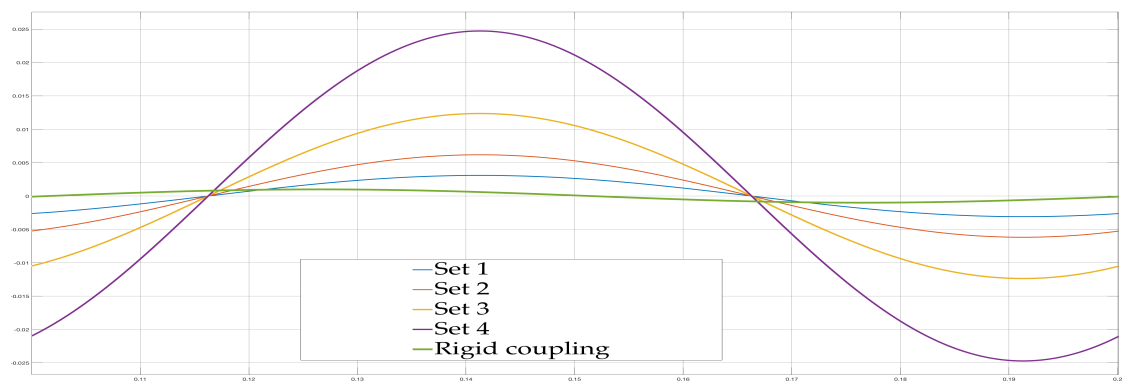
This could be accomplished, as shown before, by building an ad-hoc filter, such as fig.3 depicts, in which there are different slope profiles that will end up rejecting the disturbances at higher frequencies than the cut-off ones and preserving the signal at lower ones.

Analyzing the two opposite behaviours: **rigid coupling** and **induced virtual compliance** which is achieved through the choice of the desired cut-off frequencies (which converted in Htz are respectively equal to 8 and 80 Htz), it is interesting the comparison of the vibration suppression applied on three different noise frequencies (10^1 , 10^2 and 10^3 Htz):

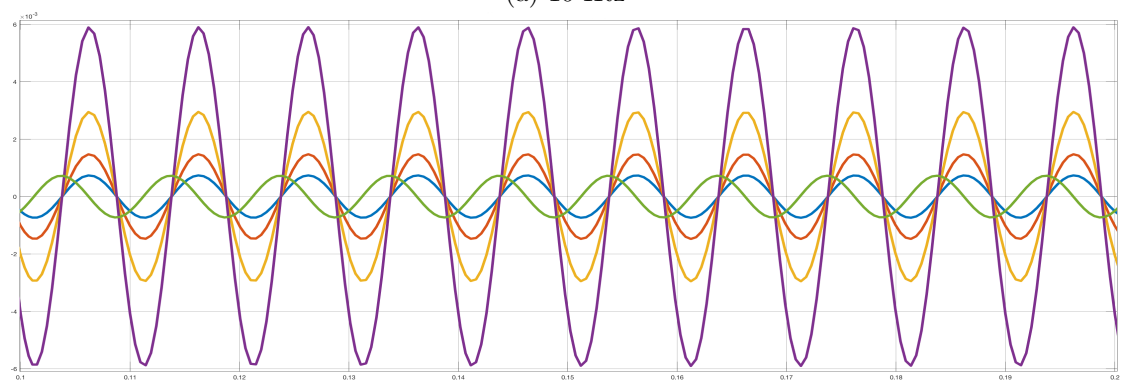
- In fig.4a is shown how the vibrations at lower frequencies are preserved by the *virtual compliance*, this is a rather desirable aspect of a teleoperation interaction since the input commands generated by the controller will have kind of low frequencies.
- The fig.4b demonstrates a turning point in which the disturbance rejection achieved

by the *rigid coupling* is comparable to the performance of the Set 1 of *virtual compliance* parameters.

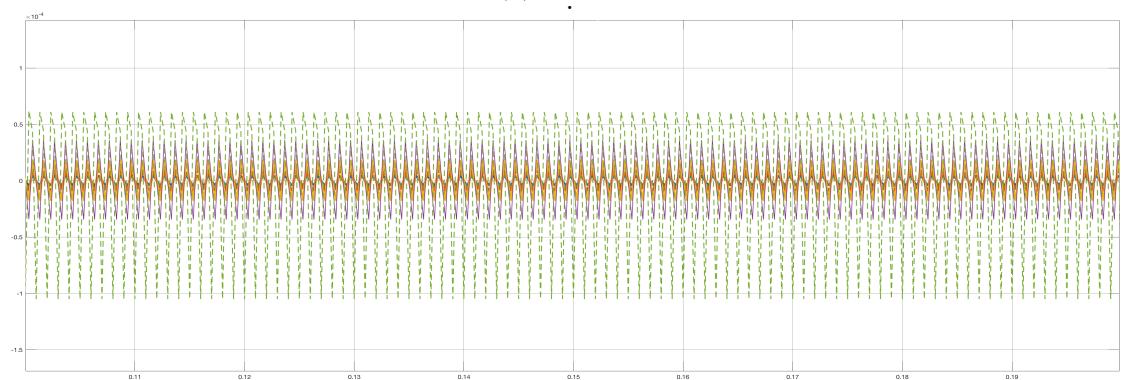
- At frequencies higher than the cut-off ones, the vibrations will be dumped more effectly by the sets of computed virtual parameters than with *rigid coupling*, this is deducible from fig.4c.



(a) 10 Htz



(b) 100 Htz



(c) 1000 Htz

Figure 4: Signal response to a noise with three different frequencies modulated by the proposed vibration damping filter.

2.2 Task execution analisys

2.2.1 Free motion with high noise frequencies

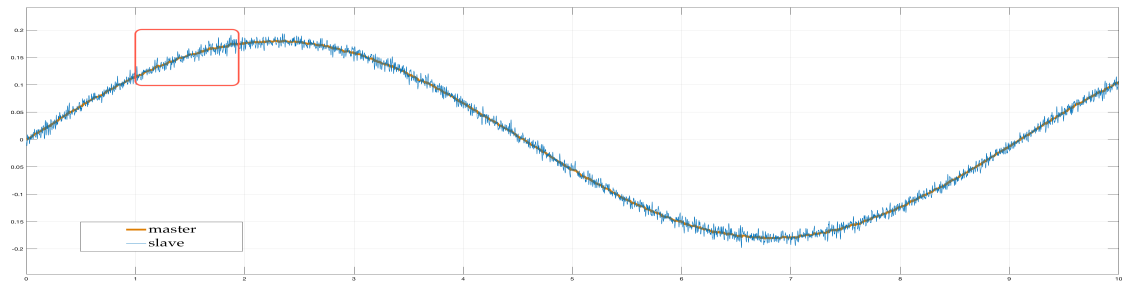
At first, we present an execution in free motion where , the slave succeeds to follow the trajectory given to the master, applying both *rigid coupling* (fig.5a) and *virtual compliance* (fig.5c), with almost no task error (without considering the error due to noise disturbances). This kind of disturbance should be damped, and in fact, using *virtual compliance* (fig.5b) the profile of the angle is smoother than in *rigid coupling* (fig.5d).

2.2.2 Free motion with low noise frequencies

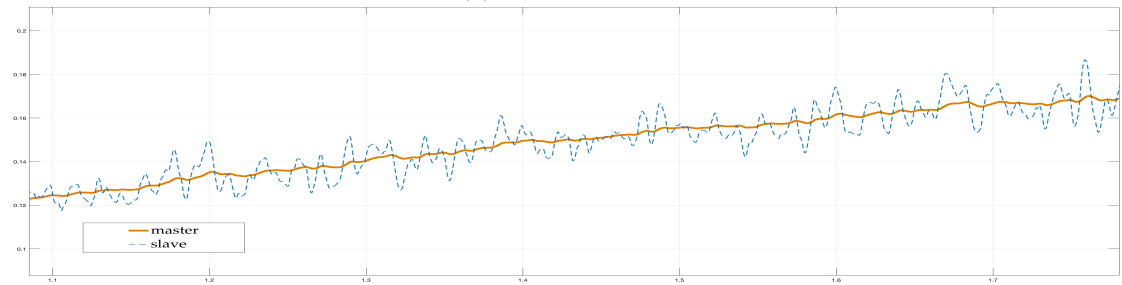
Comparatively, two other simulations have been undertaken that share the same conditions of the previous ones, if not for the noise frequency, which has been lowered. This kind of disturbance is usually a similar to the input of the control actuators, so it should be preserved, namely it shouldn't be affected by the proposed filtering. This phenomenon shows up in fig.6b and fig.6d. In fact, if compared, the two profiles confirm that *rigid coupling* cancel out most of the healthy signal, on the contrary *virtual compliance* save the signal information, which is extremely important from a control perspective.

2.2.3 Environment contact

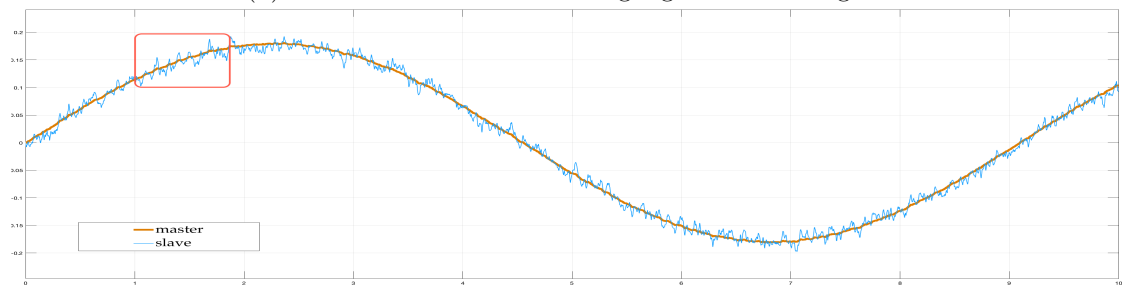
Here the proposed simulations hold the same reference trajectory for master. But, in addition, after that the slave would trespass a certaing angle value there would be a contact with the environment.



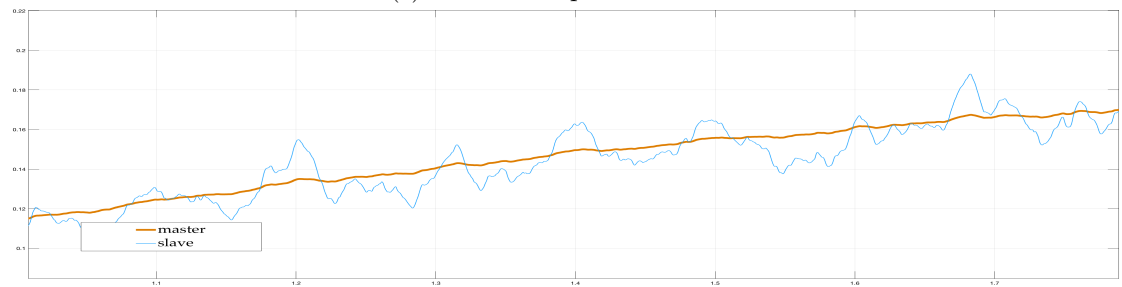
(a) Rigid coupling



(b) Particular taken from the highlighted area in fig.5a

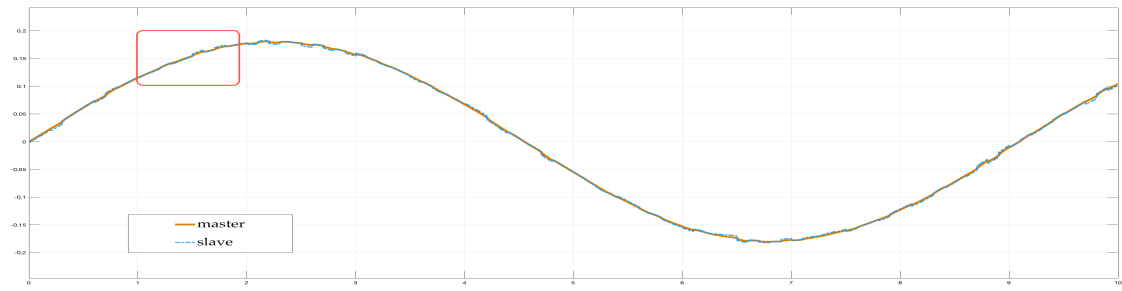


(c) Virtual compliance Set n.4

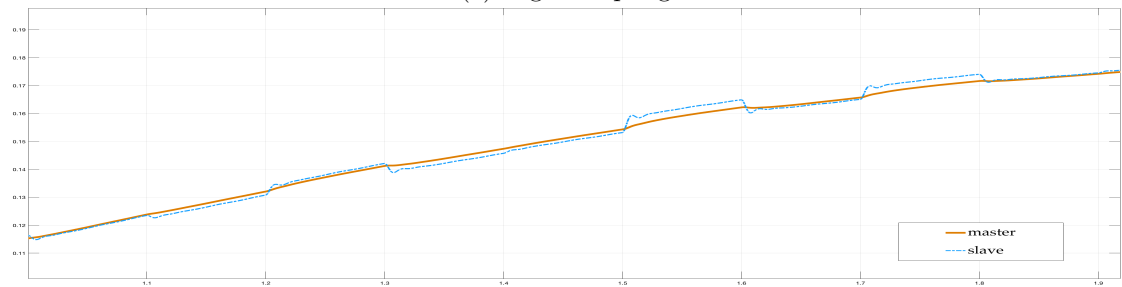


(d) Particular taken from the highlighted area in fig.5c

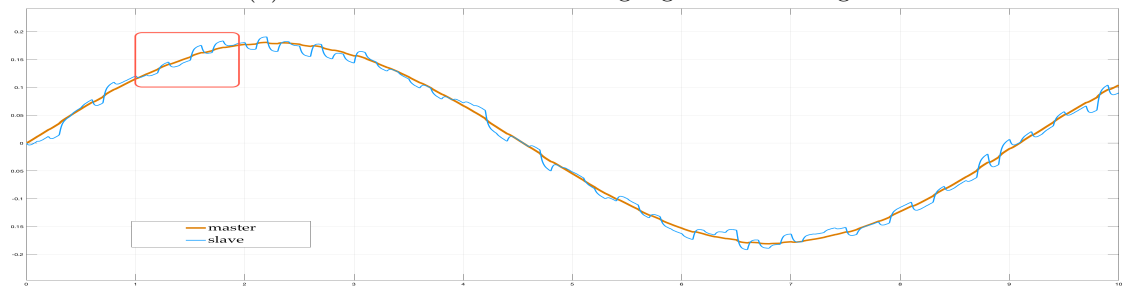
Figure 5: Free motion master-slave simulation, with artificial disturbances at 50 Htz frequency.



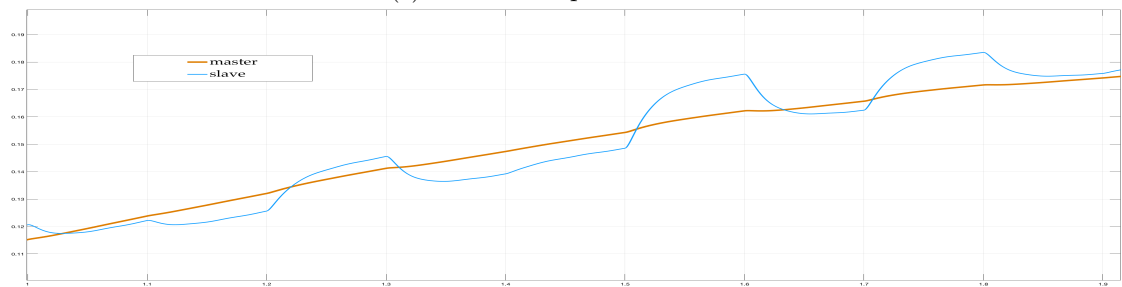
(a) Rigid coupling



(b) Particular taken from the highlighted area in fig.6a

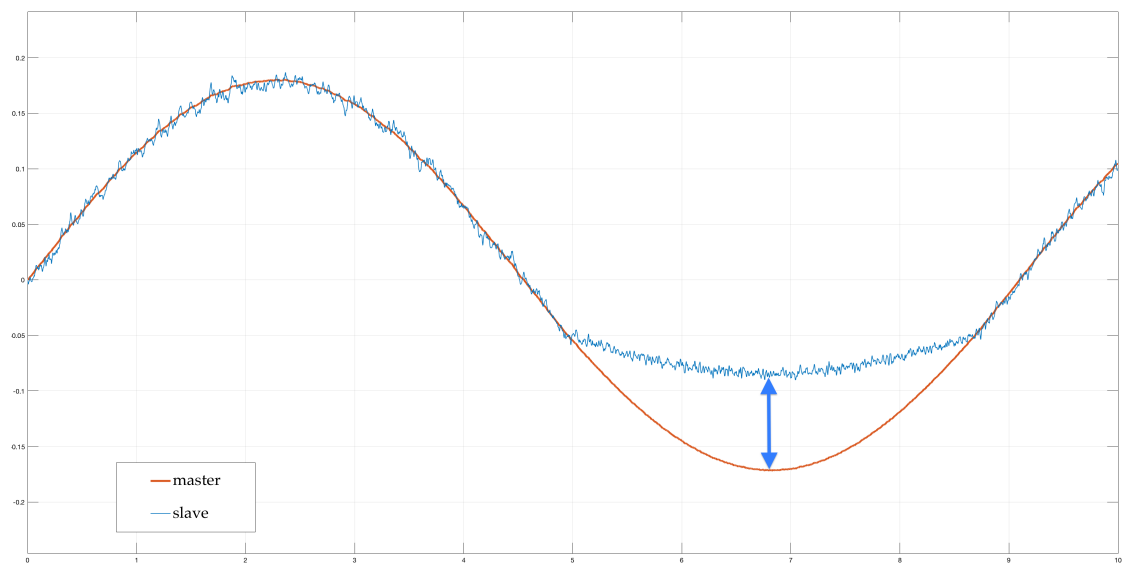


(c) Virtual compliance Set n.4

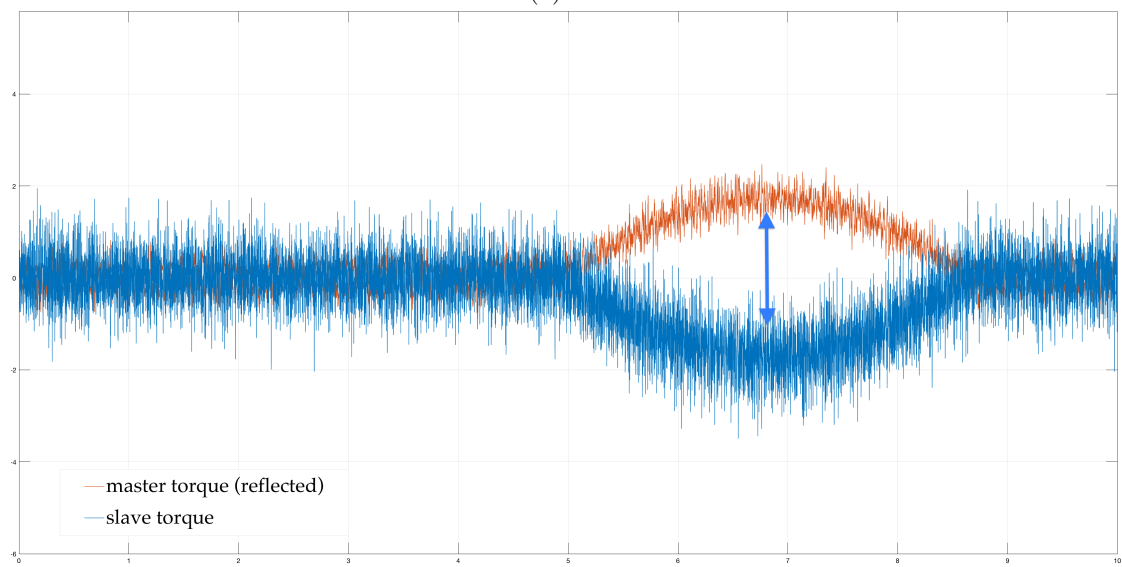


(d) Particular taken from the highlighted area in fig.6c

Figure 6: Free motion master-slave simulation, with artificial disturbances at 20 Htz frequency.

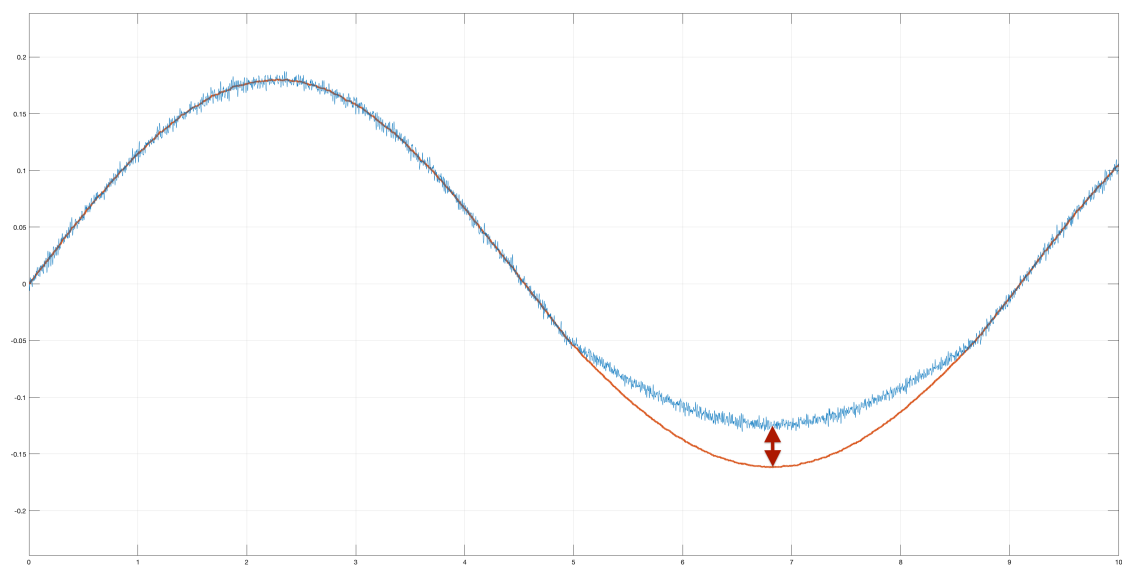


(a) ffff

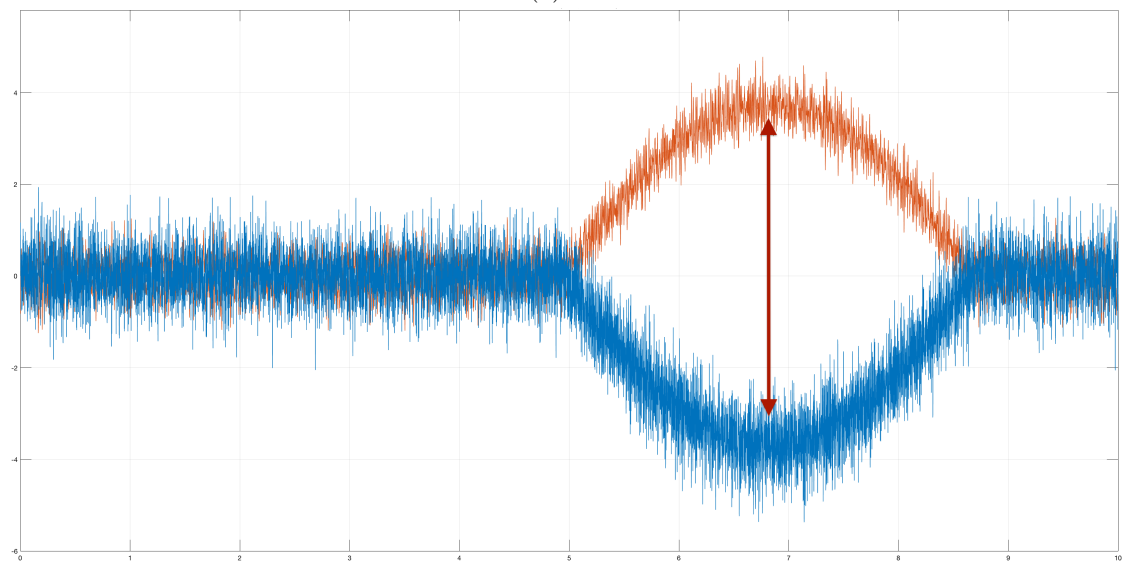


(b) ffff

Figure 7: fffff



(a) fff



(b) fff

Figure 8: ffff

3 Conclusions

References

- [1] P. F. Hokayem and M. W. Spong, “Bilateral teleoperation: An historical survey,” *Automatica*, vol. 42, no. 12, pp. 2035–2057, 2006.
- [2] C. Trakarnchaiyo and A. H. S. Abeykoon, “Vibration suppression design for virtual compliance control in bilateral teleoperation,” in *Control and Robotics Engineering (ICCRE), 2017 2nd International Conference on*, pp. 57–62, IEEE, 2017.